New Journal of Physics
The open-access journal for physics

# Dispersion properties of photonic crystal waveguides with a low in-plane index contrast

**M Augustin[1,4], R Iliew[2], C Etrich[1], F Setzpfandt[1], H-J Fuchs[1], E-B Kley[1], S Nolte[1], T Pertsch[1], F Lederer[2] and A Tünnermann[1,3]**

[1] Institute of Applied Physics, Friedrich-Schiller-Universität Jena, Max-Wien-Platz 1, 07743, Jena, Germany
[2] Institute of Condensed Matter Theory and Solid State Optics, Friedrich-Schiller-Universität Jena, Max-Wien-Platz 1, 07743, Jena, Germany
[3] The Fraunhofer Institute for Applied Optics and Precision Engineering, Albert-Einstein-Straße 7, 07745, Jena, Germany
E-mail: augustin@iap.uni-jena.de

*New Journal of Physics* **8** (2006) 210
Received 31 May 2006
Published 22 September 2006
Online at http://www.njp.org/
doi:10.1088/1367-2630/8/9/210

**Abstract.** We investigate dispersion properties of photonic crystal waveguides in a low-index material system. The modes above the light line, of a waveguide consisting of one row of missing holes (W1), exhibit high losses due to out-of-plane radiation. In contrast, the index-guided modes below the light line show moderate losses and we demonstrate both theoretically and experimentally that high dispersion is possible. Furthermore we investigate wider defect waveguides operated within the photonic band gap, where a mini-stopband with a very large suppression of transmission was found. The dispersion properties of these waveguides are discussed.

[4] Author to whom any correspondence should be addressed.


PII: S1367-2630(06)25693-3

## Contents



## 1. Introduction

In the last few years there has been an ever increasing interest in photonic crystals and photonic crystal based components, due to their potential to allow for monolithic integrated photonic devices. A basic photonic crystal based component is a waveguide which simply can be realized introducing a line defect. In contrast to conventional waveguides it shows unusual dispersion properties, viz. so-called stopbands or mini-stopbands [1]. Here, the group velocity becomes zero and thus there is no energy flux. The group index and the group velocity dispersion (GVD) can attain arbitrarily high values. The large GVD could be exploited, e.g., for dispersion compensation in fibre communication systems, where a short (centimetre scale) device could possibly replace a fibre with a length of kilometres.

So far photonic crystal-based waveguides were realized mainly in semiconductor-based slab structures such as silicon membranes [2], silicon-on-insulator [3]–[6] or GaAs-based slabs [1, 7]. More recently alternative materials like $Nb_2O_5$ [8, 9] and $Si_3N_4$ [10, 11] with a significantly lower refractive index were used. Due to the smaller refractive index the feature size is larger and efficient interfacing with standard fibres is easier to achieve. Another advantage of these materials is their wider transparency region, even going down to the visible spectral range [10, 11].

In this study, an investigation of the properties of photonic crystal waveguides realized in $SiO_2/Nb_2O_5/SiO_2$ and $SiO_2/Si_3N_4/SiO_2$ slab systems is presented and the problems arising from the lower refractive index are discussed. The slab system provides the vertical guidance via total internal reflection, and the photonic crystal consists of a hexagonal lattice of air holes. The waveguides were created by taking out consecutive rows of holes in ΓK-direction. Depending on how many (entire) rows are taken out to create the line defect, such a photonic crystal waveguide is referred to as W$n$ where $n$ corresponds to the number of rows omitted. The structures were designed to operate in the near-infrared which allows a direct comparison with high-index systems. The paper is organized as follows. First, the special design considerations for the low-index photonic crystal slab system and the fabrication procedure are discussed. The following section deals with the W1 waveguide, which is the most frequently investigated photonic crystal waveguide. Operation of the waveguide below the light line is proposed and its performance is investigated. The next section presents the experimental and theoretical results obtained for the dispersion and transmission properties of a W5 waveguide.

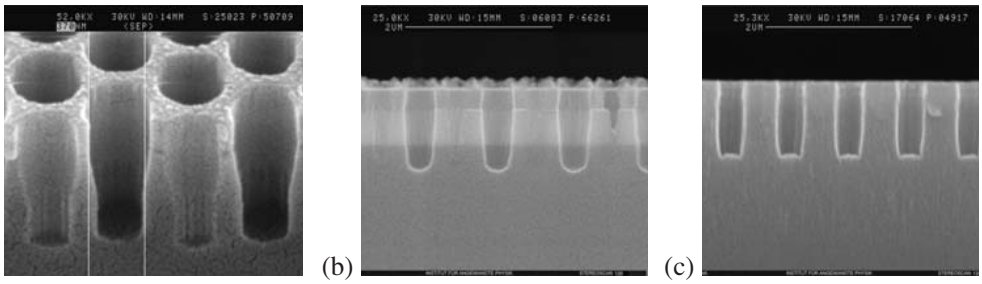

**Figure 1.** (a) and (b) SEM-images of photonic crystal samples in the $Nb_2O_5$- and (c) the $Si_3N_4$-slab system.

## 2. Design considerations, fabrication and characterization

The slab systems used here consist of a waveguiding layer of either $Nb_2O_5$ or $Si_3N_4$ (thickness $\approx$ 500 nm), sandwiched between a silica cladding (300 nm) and a silica buffer (2000 nm). This slab system is deposited on a silicon wafer which is needed to produce optical facets for efficient coupling of the excitation. The thickness of the waveguiding layer is chosen such to ensure single-mode operation in the vertical direction. The silica cladding is used to get a more symmetric structure and thus to minimize TE/TM mode-mixing.

Based on these slab systems, plane-wave bandstructure calculations were performed by means of a freely available software package [12]. As a result, the defect-free systems can exhibit an omnidirectional (in-plane) photonic bandgap where light does not propagate in the photonic crystal. If in this case a line defect is created in the photonic crystal (for instance omitting an entire row of holes) light guidance can be expected along this defect. Normally, two kinds of modes occur: modes with steep bands, which resemble the index-guided modes of conventional dielectric waveguides, and flat-band modes, which are guided by transverse Bragg reflexion and have no counterpart in conventional waveguides (gap-guidance) [13]. Otherwise, if there is no bandgap or excitations outside the bandgap, there can be only light guidance due to the difference in the index of the defect region and the effective index of the photonic crystal region (index guidance).

The photonic crystal structure of the slab systems was fabricated by means of electron beam lithography. Furthermore different etching techniques were applied depending on the slab system used. After electron beam exposure of the upper resist layer, the photonic crystal pattern was transferred into the chromium layer below. In case of the $Nb_2O_5$-slab system, a second etching mask was created in order to obtain the necessary etching depth. The slab system was then structured using either the inductive coupled plasma (ICP) or the reactive ion beam etching (RIBE) technique. Finally optical facets were obtained by cleaving and breaking the samples. Figure 1 shows scanning electron microscope (SEM)-images of cleaved optical facets for both the $Nb_2O_5$- and the $Si_3N_4$-slab systems. In both cases an etching depth of around 1 $\mu$m could be obtained.

For characterization the light of a super-luminescence diode was coupled into the sample using a lensed fibre. The light exiting the waveguides was collected with a microscope objective (40×, nuclear aperture (NA) = 0.65) and then spectrally separated and detected in an optical spectrum analyser. A reference measurement (without the sample) was performed in order to

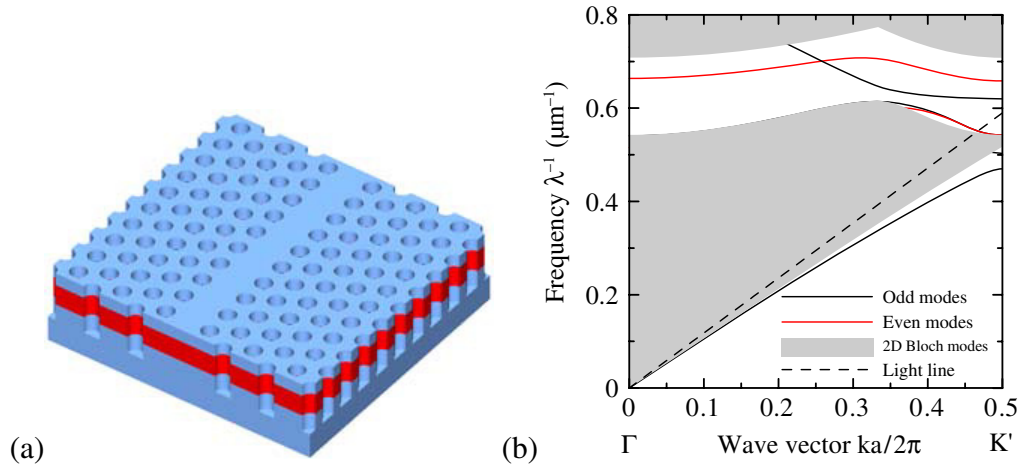


**Figure 2.** (a) Schematic drawing and (b) bandstructure of a W1 photonic crystal waveguide consisting of a triangular lattice (diameter of holes 374 nm, lattice pitch 595 nm). The grey region indicates frequencies, where light can propagate as 2D Bloch waves inside the photonic crystal without defect.

determine the spectral characteristics of the light source. In addition, for the wavelength at maximum transmission, a stray light measurement was carried out from above the sample. The stray light was collected using a microscope objective (125× long distance (LD), NA = 0.8) and projected onto an InGaAs-camera. By means of the stray light data, it is possible to determine the waveguide loss inside the photonic crystal sample directly, thus avoiding to deal with coupling losses at the optical facets or reflection losses at the interfaces of the photonic crystal waveguide and the ridge waveguides. They are used to couple light into and out of the photonic crystal waveguide.

## 3. Dispersion of W1 photonic crystal waveguides

The simplest structure is a W1 waveguide (cf figure 2(a)). First a photonic crystal structure comprising a triangular lattice of air holes with a diameter of 374 nm, a lattice pitch of 595 nm and a length of 58 $\mu$m along the ΓK-direction was realized in a $Nb_2O_5$-slab system. Ridge waveguides are used to couple light into the photonic crystal waveguide (cf figure 3(a)). The corresponding calculated two dimensional (2D) bandstructure (using an effective index) for TE-like polarization is displayed in figure 2(b). Here, only the fundamental (odd) modes, of the defect waveguide are considered, because they are easier to excite and are expected to have lower losses than the even modes. For the odd modes, gap-guiding (flat part of the band inside the bandgap) and index-guiding (steeper part of the band inside the bandgap and modes below the light line) is possible. At the edge of the Brillouin zone, the band corresponding to the gap-guided modes becomes very flat (cf figure 2(b), black solid curve), indicating that the group velocity approaches zero while the group index,

$$n_g = c\frac{dk}{d\omega} = -\frac{\lambda^2}{2\pi}\frac{dk}{d\lambda}, \tag{1}$$

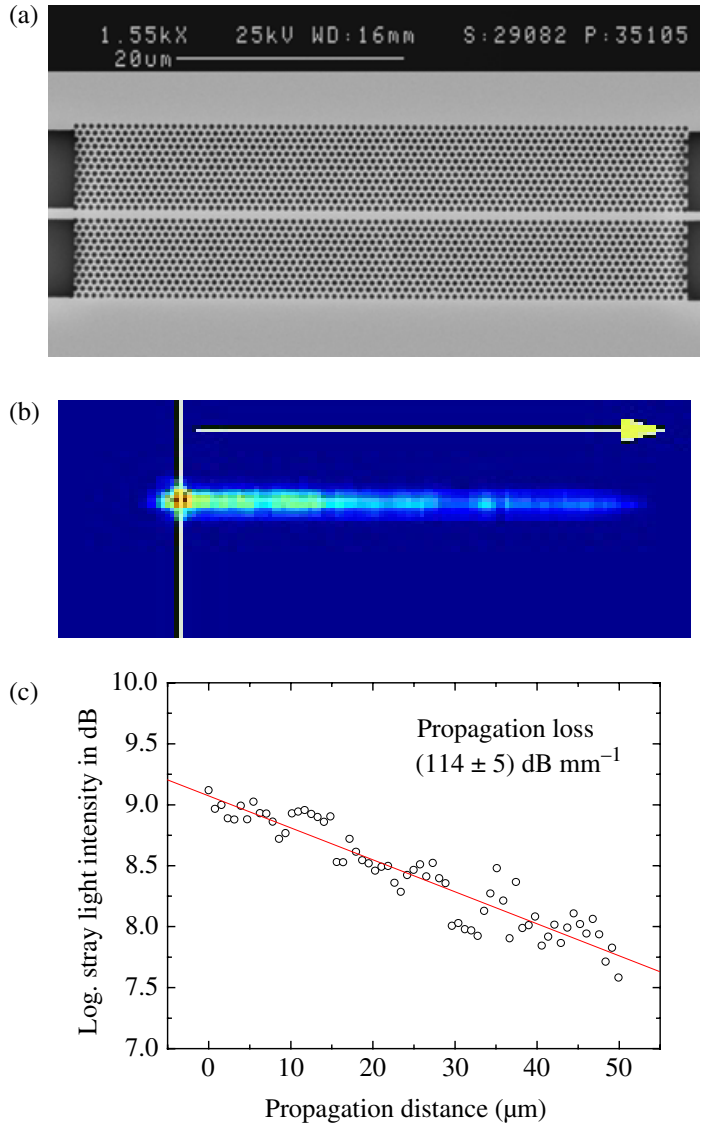


**Figure 3.** (a) SEM-image of photonic crystal waveguide sample, and (b) and (c) stray light measurement (at 1493 nm) to determine the propagation loss for TE-polarization.

diverges. This leads to a large GVD, GVD $= c^{-1}\mathrm{d}n_{\mathrm{g}}/\mathrm{d}\lambda$, of the gap-guided modes near the edge of the Brillouin zone. They establish the upper part of a mini-stopband. The lower part (outside of the 2D photonic bandgap) is index-guided. It vanishes into the continuum of 2D Bloch states and does not play a role for our consideration. Depending on the actual parameters, these modes can even be superposed almost completely by the continuum. Note, that the even modes are entirely gap-guided.

First we concentrate on the odd modes within the bandgap. Characterization of the photonic crystal waveguide yields losses of at least $(114 \pm 5)$ dB mm$^{-1}$ at a wavelength of 1493 nm (inside the photonic bandgap) in the index-guided region, where the slope of the band is large (see figure 2(b)). The losses are due to the very strong interaction of the mode with the 2D photonic

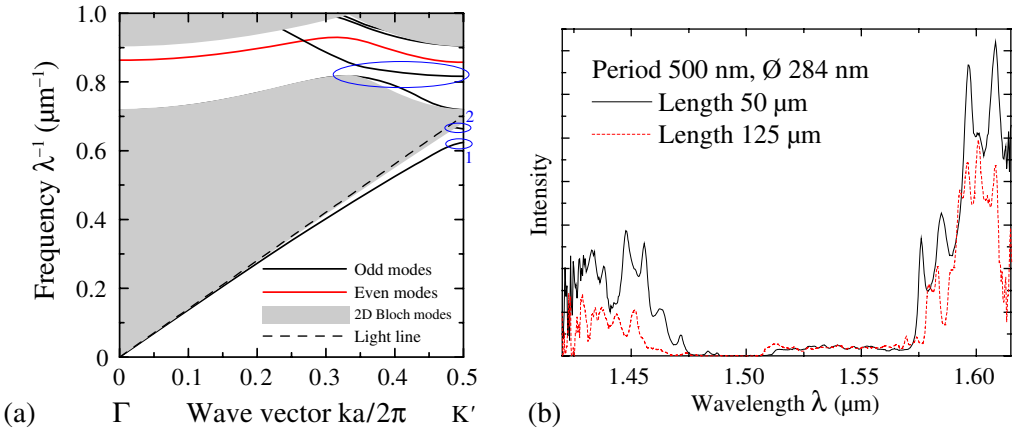


**Figure 4.** (a) 2D bandstructure and (b) experimental transmission spectrum for TE-polarization of a W1 photonic crystal waveguide (ΓK-direction, diameter of holes 320 nm, period 500 nm) based on the $Si_3N_4$-slab system. The index-guided mode lying below the light line is located at 1550 nm. The ellipses in (a) mark the regions of small group velocity and high dispersion, where 1 and 2 are below the light line.

crystal, because a major (although evanescently decaying) part of the modal energy overlaps with the cladding in such a narrow waveguide. Consequently, because the modes are above the light line, efficient out-of-plane scattering induces large propagation losses. This is confirmed by a 3D finite-difference time-domain (FDTD) simulation. On the other hand, the gap-guided part of the modes (flat region) is expected to have even larger losses due to the lower group velocity.

As mentioned above, there are also (index-guided) waveguide modes below the light line ($\lambda^{-1} < 0.5\,\mu m^{-1}$), which should lead to much lower losses. Here, the bands corresponding to the waveguide modes are again very flat. Furthermore a mini-stopband of the waveguide modes can be identified near the edge of the Brillouin zone. Thus high dispersion can be expected there as well. To access this domain with the available experimental wavelength range (around $\lambda = 1550$ nm), the structure parameters were scaled accordingly. For this purpose, we used the $Si_3N_4$-slab system since it exhibits a better structuring quality for the required photonic crystal parameters (diameter of holes 320 nm and period 500 nm). A 2D band structure (using an effective index) for these parameters is shown in figure 4(a) which looks very similar to figure 2(b). Note that the large blue ellipse in figure 4(a) marks the mini-stopband mentioned above.

SEM-images of photonic crystal waveguides with these new parameters reveal somewhat smaller holes of diameter 284 nm with a depth of 700 nm. W1 photonic crystal waveguides with lengths of 50 and 125 $\mu$m were realized. Again ridge waveguides were used to couple light into the photonic crystal waveguides.

The measured transmission spectra of the fabricated samples are shown in figure 4(b). Around 1450 and 1600 nm, there is an enhanced transmission. Detecting the stray light the propagation losses of the 125 $\mu$m long photonic crystal waveguide were determined as $(43 \pm 16)$dB mm$^{-1}$ at 1594 nm (see figure 5) which is considerably lower as in the case of modes within the bandgap which are located inside the light cone and thus radiate partially into the substrate. For the index-guided modes under consideration, this loss does not occur. It should be noted that the smaller structure sizes result in inferior structure quality and thus

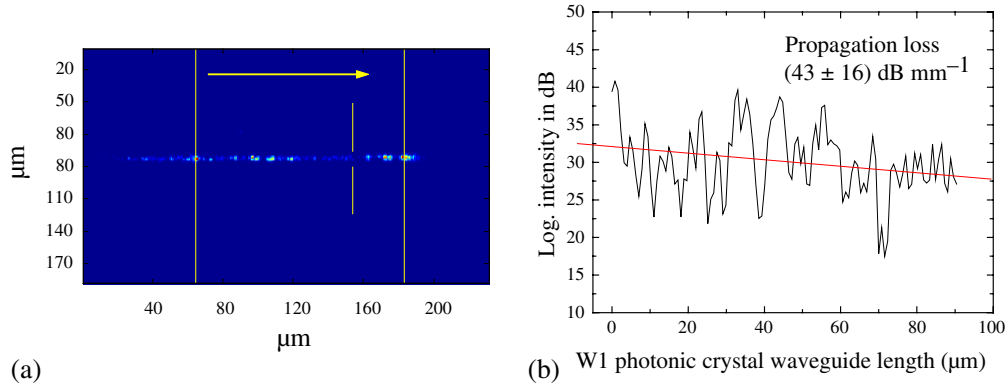


**Figure 5.** (a) Detected stray light for TE-polarization at 1594 nm along a 125 $\mu$m long W1 photonic crystal waveguide, marked with yellow lines. (b) Fit of the experimental stray light intensity.

higher scattering losses due to surface roughness. Hence structures qualitatively equivalent to the larger ones should result in even smaller losses.

Comparing the transmission spectra with the location of the waveguide bands in the band structure shows that the region of low transmission corresponds to the mini-stopband (1450–1530 nm). Since the waveguide bands are relatively flat, an increase of the group index and the GVD can be expected there. The upper band yields anomalous (GVD $> 0$) and the lower band normal dispersion (GVD $< 0$). In contrast, for the gap-guided modes investigated before only anomalous dispersion (GVD $> 0$) is possible.

Theoretical values for the group index and GVD were obtained by means of the FDTD-method. Figures 6(a) and (b) show the calculated transmission spectra for the two regions marked in 4(a) with 1 and 2, and the group index and GVD. They were determined taking respective derivatives of the spectral phase difference between input and output facet yielding very high values of up to $\pm 1\,\mathrm{ps\,nm^{-1}\,mm^{-1}} = \pm 1\,000\,000\,\mathrm{ps\,nm^{-1}\,km^{-1}}$.

The reflectivity due to the interface between the ridge and photonic crystal waveguides increases with the frequency approaching the mini-stop-band. This can be exploited to determine the group index experimentally using the formula of a Fabry–Pérot resonator:

$$n_{\mathrm{g}} = \frac{\lambda_1 \lambda_2}{2d(\lambda_2 - \lambda_1)}, \tag{2}$$

where $\lambda_1$ and $\lambda_2$ are two consecutive oscillations in the transmission spectra and $d$ is the length of the photonic crystal waveguide. In figure 7(b), the derived group index based on the spacing of the oscillations is shown. To recheck these values the measurement was repeated with a tunable laser. Although here different coupling conditions were used and a different height of the oscillation peaks was observed, the spacing in the transmission spectra was the same.

The values obtained for the group index were fitted by means of an appropriate function (see figure 7(a)). The maximum value here is around 6, for the gap-guided modes in a silicon membrane system, a group index as high as $n_g = 100$ was found [13]. Calculating the derivative of these functions with respect to the wavelength the GVD is obtained (see also figure 7). The

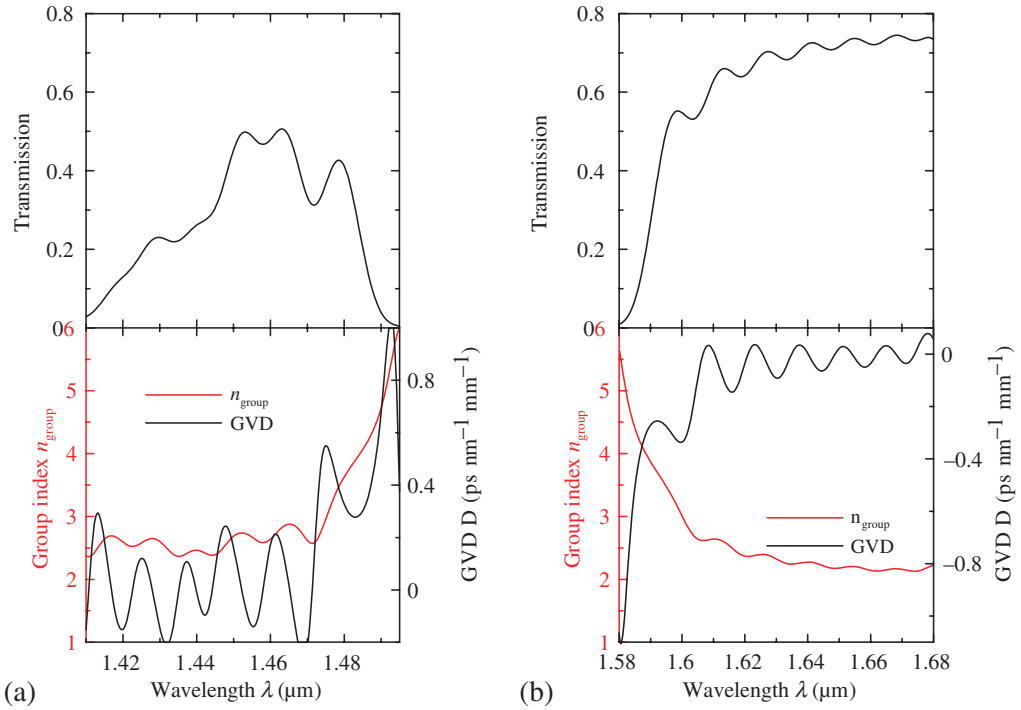


**Figure 6.** Transmission spectra, group index and GVD for the two regions with flat bands marked with (a) 2 and (b) 1 in figure 4(a).

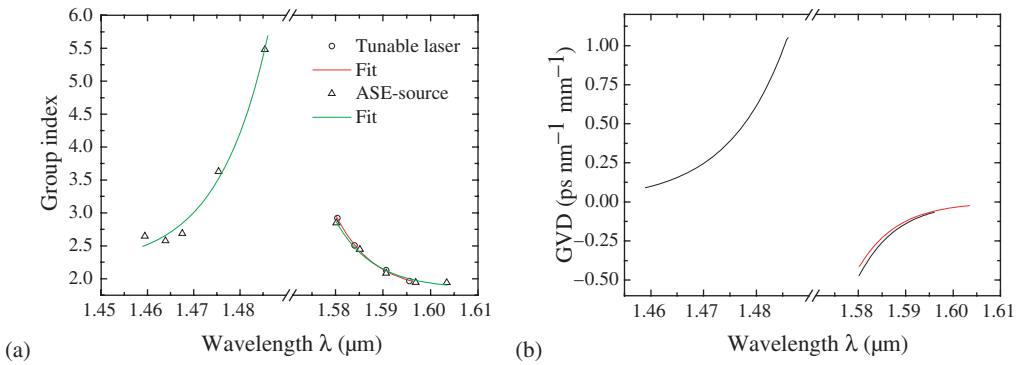


**Figure 7.** (a) Wavelength dependence of the group index determined from the experimental transmission spectra in figure 4(a). (b) GVD determined calculating the first derivative of the function fitted in (a).

largest dispersions were found to be +1 000 000 ps nm$^{-1}$ km$^{-1}$ and −500 000 ps nm$^{-1}$ km$^{-1}$. For comparison, the GVD of a silica fibre at a wavelength of 1.55 $\mu$m amounts to 17 ps nm$^{-1}$ km$^{-1}$. With such a high dispersion, only a length of 34 $\mu$m would be necessary to compensate for the dispersion of a 1 m long silica fibre.

The excitation of the index-guided mode (below the light line) of a photonic crystal waveguide is a possibility to achieve high dispersion with moderate losses without the need of a complete photonic band gap. However, at a wavelength of 1.55 $\mu$m very small structure

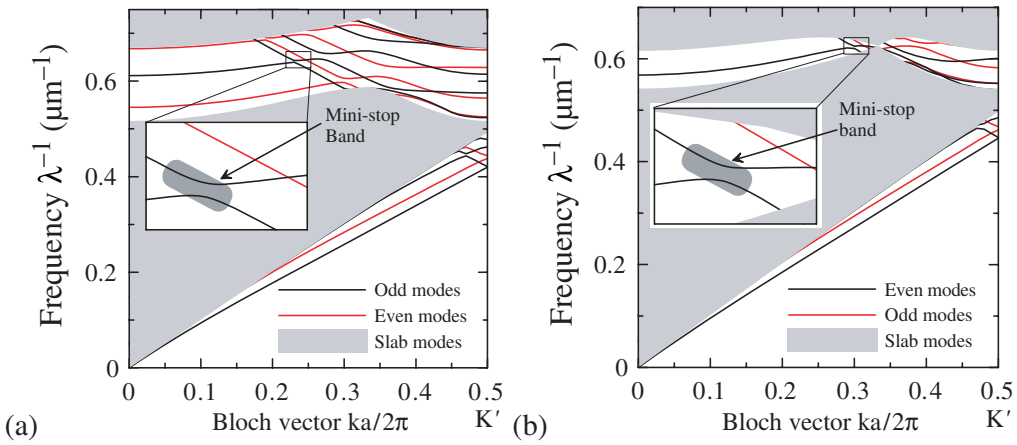


**Figure 8.** (a) Bandstructure for TE and (b) TM modes of a W5 photonic crystal waveguide (diameter of holes 380 nm, period 620 nm). The insets show the enlarged regions of interest of the respective mini-stopbands.

sizes are needed in order to use these index-guided modes. On the other side, for using the gap-guided modes of a photonic crystal waveguide, the propagation losses need to be reduced.

## 4. Dispersion of W5 photonic crystal waveguides

A simple idea to reduce the overall propagation loss inside a photonic crystal waveguide is to increase the width of the waveguide, e.g. by realising W3, W5 or even W9 waveguides, because the penetration depth of the fundamental mode into the 2D photonic crystal region is reduced, and hence the interaction is much weaker. Then, even above the light line, low-loss propagation can be expected. As pointed out above, larger structure sizes could be used operating the waveguide within the bandgap at the desired wavelength range. Much lower losses of 8.5 dB $mm^{-1}$ for the W3, 2.6 dB $mm^{-1}$ for the W5 and 1.7 dB $mm^{-1}$ for the W9 were already demonstrated [9].

Apart from lower losses, wider photonic crystal waveguides support multiple modes. This makes it more likely to find mini-stopbands within the bandgap to exploit the unusual dispersion properties in the bandgap region [6, 14]. Calculating the 2D bandstructure for a W5 photonic crystal waveguide ($Nb_2O_5$-slab system with diameter of holes 380 nm and period 620 nm) the existence of a mini-stopband within the bandgap in this low in-plane index-contrast system can be confirmed for TE-polarization (around $\lambda^{-1} = 0.641\,\mu m^{-1}$, $\lambda = 1560$ nm, see figure 8(a)). For TM-polarization, a mini-stopband can be expected at 1616 nm (see figure 8(b)). But there is no complete bandgap in this case. Since a mini-stopband is essentially an anticrossing of modes, the bands of the waveguide modes are becoming very flat in the vicinity of the mini-stopband and therefore high dispersions can be expected there.

Based on the above parameters W5 photonic crystal waveguides were fabricated. SEM images of the optical facet show deeply etched holes with a depth of 1200 nm and an average diameter of 380 nm. To be sure to meet the design goal, in this case also photonic crystal waveguides were fabricated using a larger exposure dosage resulting in larger hole diameters. SEM-images show that these holes have diameters of 406, 430 and 453 nm. Thus there was a possibility to investigate how the stopband wavelength changes with the hole diameter. After

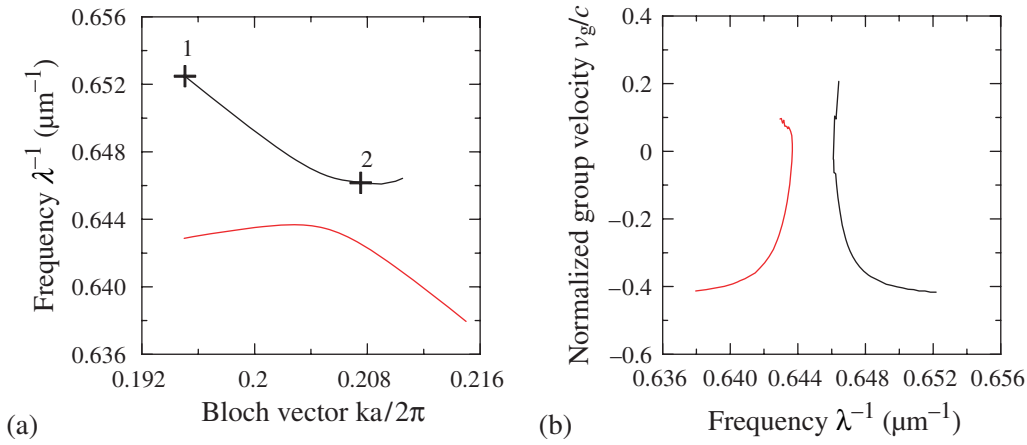


**Figure 9.** (a) Mini-stopband region (inset in figure 8(a)) obtained from full 3D FDTD calculations and (b) respective group velocity for a W5 waveguide (diameter of holes 453 nm, period 620 nm). The symbols are explained in the text.

cleaving, W5 photonic crystal waveguides with a length of 4 mm were obtained and characterized for both polarizations.

For quantitative comparison, for one of these samples the bandstructure in the mini-stopband region was calculated by means of 3D FDTD simulations using Bloch boundaries in propagation direction and open boundaries (perfectly matched layers) in the direction perpendicular to the waveguide, avoiding thus errors from the effective index approximation (see figure 9(a)). The size of the gap is 6 nm, centred at 1.551 $\mu$m. The group velocity was obtained from the first derivative (see figure 9(b)). However, the region of reduced group velocity has a bandwidth of 15 nm (figure 9(b)).

First we compared the wavelength dependence of the propagation loss for the four different hole diameters. The peaks in the propagation loss can be attributed to mini-stopbands (figure 10(a)). They shift towards larger wavelengths for smaller hole diameters. The lowest propagation loss could be determined as 2.6 dB mm$^{-1}$ for the W5 photonic crystal waveguide with a hole diameter of 453 nm. This value is in excellent agreement with previous investigations of wide photonic crystal waveguides [8]. The absolute mini-stopband suppression was too high to be measurable, since after a propagation length of 4 mm only background noise was observed.

Figure 10(b) shows a direct comparison between TE-and TM-polarization for the W5 photonic crystal waveguide with a hole diameter of 453 nm showing a significant shift of approximately 100 nm. For TE-polarization, the smallest attenuation is 2.6 dB mm$^{-1}$ and for TM polarization 4.3 dB mm$^{-1}$. In order to estimate the overall suppression of the mini-stopband, 3D FDTD transmission simulations for a finite length waveguide were performed in this case. Figure 11 shows an excellent agreement of the mini-stopband location between experiment and theory, with a difference of less than 5 nm. Also the agreement with the gap location in figure 9 is excellent. Moreover, one can note (from both the experimental and the theoretical loss curve) that the bandwidth of reduced transmission is larger than just the modal gap (6 nm), but corresponds to the region of reduced group velocity (15 nm).

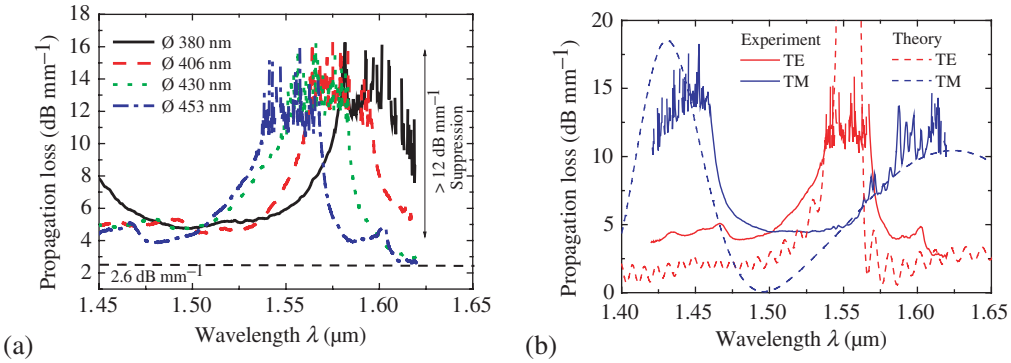


**Figure 10.** (a) Wavelength dependence of the propagation loss for W5 photonic crystal waveguides with different hole diameters ranging from 380 to 453 nm (TE-polarization) and (b) for the W5 with hole diameter 453 nm (TE- and TM-polarization). A shift of the position of the mini-stopband in dependence on the hole diameter was detected.

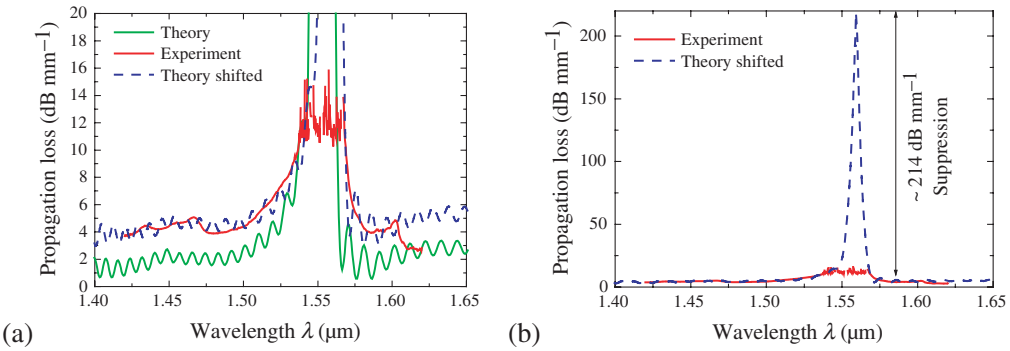


**Figure 11.** (a) and (b) Comparison between calculated and measured propagation loss of the W5-photonic crystal waveguide with a hole diameter of 453 nm. The fringes in the theoretical spectrum are due to reflections at the boundaries of the computational window. Note that panels (a) and (b) are scaled differently.

By comparing the calculated propagation losses with the experiment, we observed approximately 2.5 dB mm$^{-1}$ higher losses in the experiments, due to material scattering losses. Since the slab losses amount to around 0.4 dB mm$^{-1}$, these losses are mainly attributed to remains of the polymer etching mask. Since the FDTD transmission spectra, shifted by 2.5 dB mm$^{-1}$ in order to incorporate the high scattering losses, are an excellent fit of the experimental data, the mini-stopband suppression can be estimated to amount to approximately 200 dB mm$^{-1}$.

Since the TE-propagation losses of the W5 are approximately 3–4 dB mm$^{-1}$ and the estimated mini-stopband suppression amounts to 200 dB mm$^{-1}$, 10 times shorter waveguides (400 $\mu$m) would still produce significant suppression effects (around 20 dB) while allowing for reasonable transmissions of around 0.4 dB outside the mini-stopband. At this length, the FWHM-bandwidth of the mini-stopband would amount to around 15 nm. With this performance, the

application of W5 photonic crystal waveguides as a notch filter with a narrow bandwidth and high suppression is possible.

The high transmission of the W5 waveguide outside the mini-stopband may suggest to exploit the dispersion of the waveguide at an even higher transmission than for the W1. However, as already discussed, the bandwidth of reduced transmission (15 nm) is much larger than the modal gap itself, meaning that here already in the vicinity of the gap the transmission is low. This can be attributed mainly to two facts. Firstly, the modal shape changes drastically approaching the mini-stopband. The previously index-guided fundamental (steep band) mode transforms into a gap-guided higher order zigzag (flat band) mode with strong transverse modulation. Hence, the modal (impedance) mismatch to the ridge waveguide mode is high. Secondly, this higher order mode, in contrast to the fundamental, now strongly interacts with the photonic crystal cladding, leading to high out-of-plane scattering losses, because it is located above the light line. Inspecting the imaginary part of the frequency eigenvalues from the FDTD bandstructure calculations, an increase of the out-of-plane loss by a factor of 4.5 was obtained when the group velocity was reduced from $0.42c$ (symbol 1 in figure 9(a), here 2.5 dB mm$^{-1}$ loss) to $0.31c$, and even a factor of 11 was found for going from $0.42c$ to $0.07c$ (symbol 2 in figure 9(a)) corresponding to a theoretical value of 28 dB mm$^{-1}$, whereas below the light line these losses would not occur. Thus for the W5 operated above the light line, already close to the mini-stopband the propagation losses are prohibitive for utilising the large waveguide dispersion.

## 5. Conclusions

We have investigated both theoretically and experimentally dispersion properties of photonic crystal waveguides in a low-index material system. The transparent region of this material system extends to the visible spectral range. However, in order to allow for comparison of our results with semiconductor photonic crystal waveguides discussed in the literature, all photonic crystal samples were designed to operate in the near infrared. Operating W1 photonic crystal waveguides within the bandgap leads to very high losses which is due to the waveguiding modes being located above the light line. This results in large out-of-plane losses, which is a direct consequence of the small refractive index-contrast. In contrast, operating the W1 waveguide within an index-guided region located below the light line (and below the photonic bandgap) leads to considerably smaller losses. We demonstrated that a dispersion of up to $\pm 1\,000\,000$ ps nm$^{-1}$ km$^{-1}$ is possible here. Since the losses are caused by an inferior structure quality due to smaller structure sizes, a better structure quality should thus allow for a significant reduction. Finally, we investigated in more detail wider defect waveguides operated within the photonic band gap. Apart from lower losses, we found a mini-stopband with a very large suppression (200 dB mm$^{-1}$) allowing the realization of 400 $\mu$m long devices with a 15 nm wide filtering property (20 dB) and very small losses outside the band filter (0.4 dB). However, theoretical investigations revealed, that these mini-stopbands above the light line cannot be used for dispersion compensation due to the highly increased out-of-plane loss.

## Acknowledgments

We gratefully acknowledge support by the Federal Ministry of Education and Research (Unternehmen Region, ZIK) and the Deutsche Forschungsgemeinschaft within the framework of the priority programme ‘Photonic Crystals’.

## References


[1] Olivier S, Rattier M, Benisty H, Weisbuch C, Smith C J M, De La Rue R M, Krauss T F, Oesterle U and Houdré R 2001 Mini-stopbands of a one-dimensional system: the channel waveguide in a two-dimensional photonic crystal *Phys. Rev.* B **63** 113311

[2] Herrmann R, Sünner T, Hein T, Löffler A, Kamp M and Forchel A 2006 Ultrahigh-quality photonic crystal cavity in GaAs *Opt. Lett.* **31** 1229

[3] Chutinan and Noda S 2000 Waveguides and waveguide bends in two-dimensional photonic crystal slabs *Phys. Rev.* B **62** 4488

[4] Notomi M, Shinya A, Yamada K, Takahashi J, Takahashi C and Yokohama I 2002 Structural tuning of guiding modes of line-defect waveguides of silicon-on-insulator photonic crystal slabs *IEEE J. Quantum Electron.* **38** 736

[5] McNab S J, Moll N and Vlasov Y A 2003 Ultra-low loss photonic integrated circuit with membrane-type photonic crystal waveguides *Opt. Express* **11** 2927

[6] Loncar M, Nedeljkovic D, Pearsall T P, Vuckovic J, Scherer A, Kuchinsky S and Allan D 2002 Experimental and theoretical confirmation of Bloch-mode light propagation in planar photonic crystal waveguides *Appl. Phys. Lett.* **80** 1689

[7] Talneau A, Mulot M, Anand S and Lalanne P 2003 Compound cavity measurement of transmission and reflection of a tapered single-line photonic-crystal waveguide *Appl. Phys. Lett.* **82** 2577

[8] Augustin M, Fuchs H-J, Schelle D, Kley E-B, Nolte S, Tünnermann A, Iliew R, Etrich C, Peschel U and Lederer F 2003 Highly efficient waveguide bends in photonic crystal with a low in-plane index contrast *Opt. Express* **11** 3284

[9] Augustin M, Fuchs H-J, Schelle D, Kley E-B, Nolte S, Tünnermann A, Iliew R, Etrich C, Peschel U and Lederer F 2004 High transmission and single-mode operation in low-index-contrast photonic crystal waveguide devices *Appl. Phys. Lett.* **84** 663

[10] Augustin M, Schelle D, Fuchs H-J, Nolte S, Kley E-B, Tünnermann A, Iliew R, Etrich C, Peschel U and Lederer F 2005 Self-guiding of infrared and visible light in photonic crystal slabs *Appl. Phys.* B **81** 313

[11] Crozier K B, Lousse V, Kilic O, Kim S, Fan S and Solgaard O 2006 Air-bridged photonic crystal slabs at visible and near-infrared wavelengths *Phys. Rev.* B **73** 115126

[12] Johnson S G and Joannopoulos J D 2001 Block-iterative frequency-domain methods for Maxwell's equations in a planewave basis *Opt. Express* **8** 173

[13] Notomi M, Yamada K, Shinya A, Takahashi J, Takahashi C and Yokohama I 2001 Extremely large group-velocity dispersion of line-defect waveguides in photonic crystal slabs *Phys. Rev. Lett.* **87** 253902

[14] Olivier S, Benisty H, Weisbuch C, Smith C J M, Krauss T F and Houdré T 2003 Coupled-mode theory and propagation losses in photonic crystal waveguides *Opt. Express* **11** 1490